Chemistry and Mechanism of Alizarin Red S and Methylene Blue Biosorption onto Olive Stone: Equilibrium and Kinetic

Albadarin, A. B., & Mangwandi, C. (2015). Chemistry and Mechanism of Alizarin Red S and Methylene Blue Biosorption onto Olive Stone: Equilibrium and Kinetic. Paper presented at The Third Internation Conference on Water, Energy and Environment (ICWEE), Sharjah, United Arab Emirates.

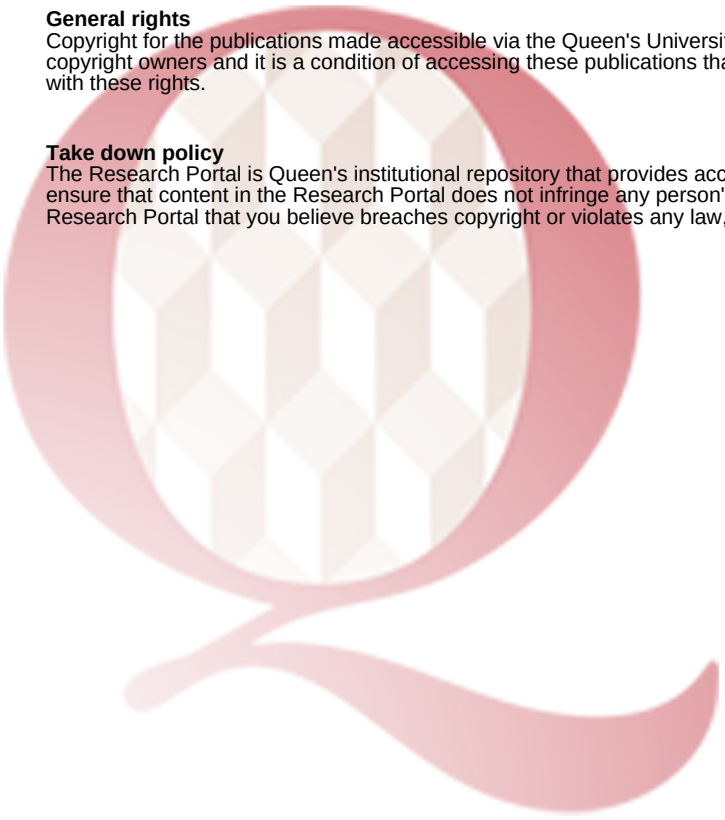

Chemistry and Mechanism of Alizarin Red S and Methylene Blue Biosorption onto Olive Stone: Equilibrium and Kinetic

Ahmad B. AlbadarinSynthesis & Solid State Pharmaceuticals Center (SSPC), Department of Chemical and Environmental Science, University of Limerick, Ireland (Ahmad.B.Albadarin@ul.ie)
Chirangano Mangwandi [1]Sch. of Chemistry and Chemical Engineering, Queen's University Belfast, Belfast BT9 5AG, Northern Ireland UK (C.Mangwandi@qub.ac.uk)

ABSTRACT

The biosorption process of anionic dye Alizarin Red S (ARS) and cationic dye methylene blue (MB) as a function of solution pH, initial concentration and contact time onto olive stone (OS) biomass has been investigated. The main objectives of the current study are to: (i) study the chemistry and the mechanism of ARS and MB biosorption onto olive stone and the type of OS–ARS, MB interactions occurring, (ii) study the biosorption equilibrium and kinetic experimental data required for the design and operation of column reactors. Equilibrium biosorption isotherms and kinetics were also examined. Experimental equilibrium data were fitted to four different isotherms by non-linear regression method, however, the biosorption experimental data for ARS and MB dyes were well interpreted by the Temkin and Langmuir isotherms, respectively. The maximum monolayer adsorption capacity for ARS and MB dyes were 109.0 and 102.6 mg/g, respectively. The kinetic data of the two dyes could be better described by the pseudo second-order model. The data showed that olive stone can be effectively used for removing dyes from wastewater.
Keywords: anionic dye Alizarin; cationic dye methylene blue; biosorption; olive stone.

1. INTRODUCTION

The disposal of wastewaters from different industries, for example textile, leather, plastics, and cosmetics, gets a great attention by environmentalists. Untreated or partly treated industrial effluents discharged in to the natural ecosystems create a serious problem to the environment. Dye wastewater from textile and dyestuff industries is one of the most difficult waters to treat as the colour tends to hold strong even after the conventional removal processes [1]. There are more than 100,000 commercially available dyes with over 700,000 tons produced annually [2]. The presence of some of these dyes even in very small amounts i.e. < 1 mg.dm^{-3} is undesirable [3, 4]. Biosorption has received considerable attention as it has the potential to become an efficient, clean and cheap technology for the treatment of wastewater. Therefore, the main objectives of the current study are to: (i) study the chem-istry and the mechanism of ARS and MB biosorption onto olive stone and the type of OS–ARS, MB interfaces occurring and study the biosorption equilibrium and kinetic experimental data required for the design and operation of column reactors. The effect of various process parameters such as, solution pH (2–9), initial concentration (5–105 mg /dm^3) and contact time were performed.

2. MATERIALS AND METHODS

Olive stone (OS) was provided by an oil extraction plant "Cooperativa Nuestra Señoradel Castillo" located in Vilches, province of Jaen (Spain). The biomass was washed several times with distilled water and dried at 110 ºC. Full and comprehensive characterization of OS can be found in a previous investigation [5]. Main properties are: surface area = 0.16 m^2/g, total pore volume = 1.84×10^{-3} cc/g and point of zero charge = 5.17. Chemical analysis: C: 52.34%; S: <0.1%; H: 7.11%; N: 0.03% and O: 40.47%. Total titratable sites = 6.94×10^{-5} mol/g[1]. Methylene blue (319.8 g/mol) and Alizarin red S (342.2 g/mol) were purchased from Sigma Aldrich, UK. Synthetic dye solutions used in the experiments were prepared with distilled water (resistivity 18.24 Ω cm). Concentrations were measured using a UV–VIS spectrophotometer (Perkin Elmer LAMBDA 25, UK) at maximum wavelengths of λ_{max} = 668 for MB and λ_{max} = 420–520 for ARS. The experiments of MB and ARS biosorption from aqueous solutions were carried out in a series of 50 mL glass jars; samples have been regularly shaken (mechanical shaker, GerhardT type LS 5) at 100 rpm and 20 °C for 4 days to ensure reaching the equilibrium. The effect of initial solution pH on the removal of MB and ARS was examined in the range of 2–9, containing 25 cm^3 of dye solution with C_o of 110 mg/dm^3 and a biomass dosage of 1.0 g/dm^3. The pH was altered using0.1 M HCl or 0.1 M NaOH. The same procedures were employed to investigate the effect of contact time and biosorption isotherms. For the biosorption isotherm studies in single and binary systems, C_o = 5−105 mg/dm^3 for MB and ARS were used. The initial concentrations ranging from 30 to 205 mg/dm^3 for MB and ARS were employed for the contact time experiment.

ARS and MB uptake and percentage of removal were calculated according to Eqs. (1) and (2), respectively:

$$q = \left[\frac{C_o - C_e}{M}\right]\times V \qquad (1)$$

$$\text{The percentage removal} = \left[1 - \frac{C_e}{C_o}\right]\times 100\% \qquad (2)$$

where C_o and C_e are the initial and equilibrium concentration of ARS and MB in mg/dm^3, M is the amount of dry biomass in g and V is the volume of the ARS/MB solution in dm^3.

3. RESULTS AND DISCUSSION

3.1. pH effect

The solution pH plays a significant role in the chemistry of both the OS and dye molecules and has a major effect on electrostatic charges that are impart by ionized dye molecules. As can be seen in Figure 1, the removal of ARS and MB from aqueous solution is greatly dependent on the pH of the solution. The results show a maximum adsorption of ARS between pH 2 and 7. At pH above 7, the amount of ARS noticeably decreases following a typical anionic adsorption behaviour [6]. For anionic dye, ARS, the adsorption capacity decreased from 76.21 to 6.651 mg/g when the pH increased from 2 to 8. This is predominantly attributed to the deprotonation of the biosorbent surface and the presence of excess OH^- ions competing with ARS dye for the biosorption sites.

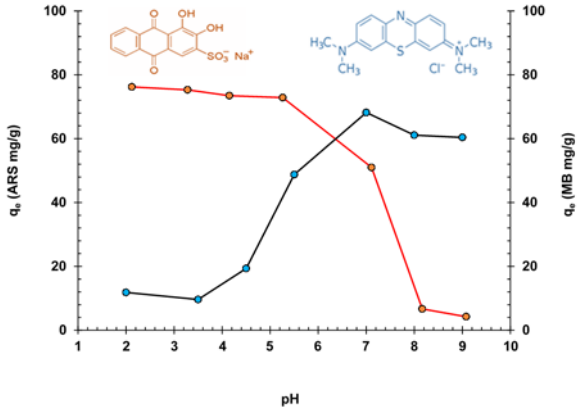

Figure 1: Adsorption of Alizarin Red S (ARS) and Methylene Blue (MB) onto olives stone as a function of pH. Experimental conditions: C_o = 110 mg/dm^3; volume 25 cm^3; biosorbent dose 1.0 g/dm^3; and shaking speed 100 rpm for 4 days.

On the other hand, opposite trends were observed for cationic dye, MB. The adsorbed amount of MB increased with increasing the pH of MB solution i.e. the maximum adsorption capacity of MB was 68.19 mg/g, observed at pH 7.25. These trends could also be well explained by the electrostatic interaction between the negatively charged surfaces of the biosorbent, at pH >pH_{PZC}, and the cationic dye.

3.2. Isotherm Experiments

The interaction between the adsorbent and the adsorbate can be understood by carrying out isotherm studies. The isotherm provides the correlation between the concentration of the adsorbate in solution and the amount of adsorbate in solid phase when both phases are in equilibrium. Figure 2 shows the equilibrium isotherms of ARS and MB dyes onto olive stone adsorbent.

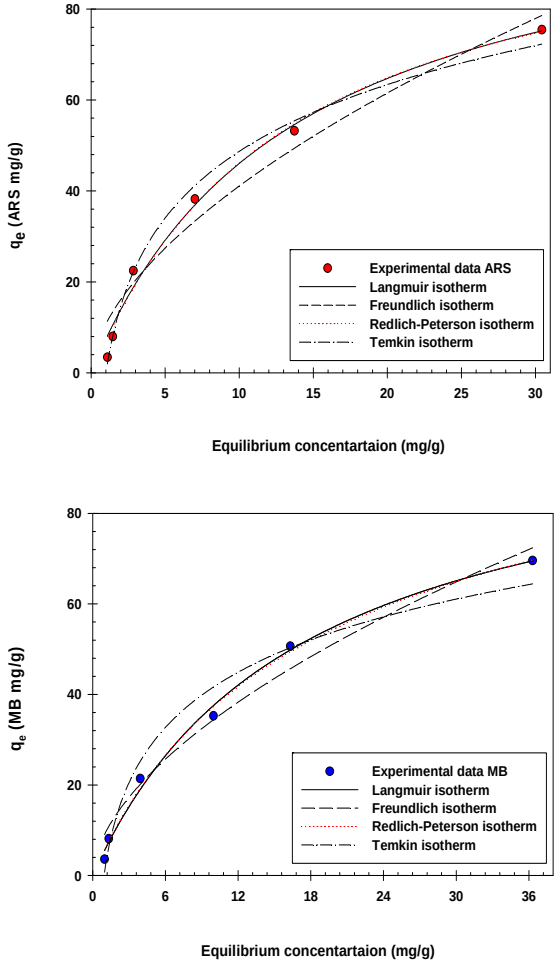

Figure 2: Non-linear forms biosorption isotherm plots of ARS and MB biosorption onto OS.

Langmuir, Freundlich, Redlich-Petersonand and Temkin isotherms were applied to the experimental data using non-linear regression in SigmaPlot Version 11 and the summary of the fits is presented in Table 1. The data presented in the table shows that Langmuir (R^2 = 0.995) and the Redlich-Peterson (R^2 = 0.992) isotherms are best models for describing the adsorption of MB onto olive stone. For ARS dye the Temkin isotherm (R^2 = 0.993) give the best description of the experimental data. According to Table 1, the olive stone has monolayer Langmuir adsorption capacities of approximately 109.0 and 102.6 mg/g for ARS and MB respectively. The adsorption capacities for the two models are similar. Table 2 shows comparison between the adsorption capacities of ARS and MB dyes with earlier studies [7-17]. The adsorption capacities of MB and ARS on olive stone are higher than most of the materials from earlier investigations.

Table 1. The Langmuir, Freundlich, Redlich-Peterson and Temkin parameters and correlation coefficients for ARS and MB adsorption onto olive stone.

Model	Parameters	ARS	MB
Langmuir isotherm $q_e = \frac{q_{max} b C_e}{1 + b C_e}$	q_{max} (mg/g)	109.0	102.6
	b (L/mg)	0.073	0.058
	R_{adj}^2	0.985	0.995
Freundlich isotherm $q_e = K_F C_e^{1/n}$	K_F (mg/g (L/mg)$^{1/n}$)	10.73	9.161
	$1/n$	0.583	0.575
	R_{adj}^2	0.953	0.978
Redlich-Peterson isotherm $q_e = \frac{K_R C_e}{1 + a_R C_e^{\beta}}$	K_R (L/mg)	7.750	6.397
	a_R ((L/mg)$^{1/\beta}$)	0.062	0.084
	B	1.033	0.925
	R_{adj}^2	0.981	0.992
Temkin isotherm $q_e = \frac{RT}{b_T} \ln A_T C_e$	A_T (L/g)	0.997	1.065
	b_T	115.0	138.1
	R_{adj}^2	0.993	0.964

Table 2: Comparison of adsorption capacities of ARS and MB with results from previous studies

Material	Adsorbate		Reference
	ARS [mg/g]	MB[mg/g]	
Olive Stone	109.30	102.60	This work
Rice Husk	-	40.59	[9]
Teawaste	-	85.16	[14]
Teawaste & Dolomite		150.00	[8]
Clay	-	58.20	[11]
Silica		11.21	[12]
M-MCCNT		48.08	[7]
Fe(III)Cr(III) hydroxide			[13]
MMT/$CoFe_2O_4$ composite		97.75	[7]
Raw date pits		27.27	[9]
Activate Date pits		80.29	[9]
Mesoporous hybrid gels	9.06 mmol/dm^3	-	[16]
Porous Xerogels	8.30mmol/kg	-	[15]
MWCNT	161.29	-	[10]
Orange peel	-	18.6	[13]

3.3. Kinetic Experiment

The pseudo first-order model equation is given as follow:

$$q_t = q_e\left(1 - e^{-k_1 t}\right) \quad (3)$$

The pseudo second-order equation is given as;

$$q_t = \frac{k_2 q_e^2}{\left(1 + k_2 q_e t\right)} t \quad (4)$$

Where k_1 (1/min) and k_2 (g/mg min) are the rate constants for first order and second-order models.

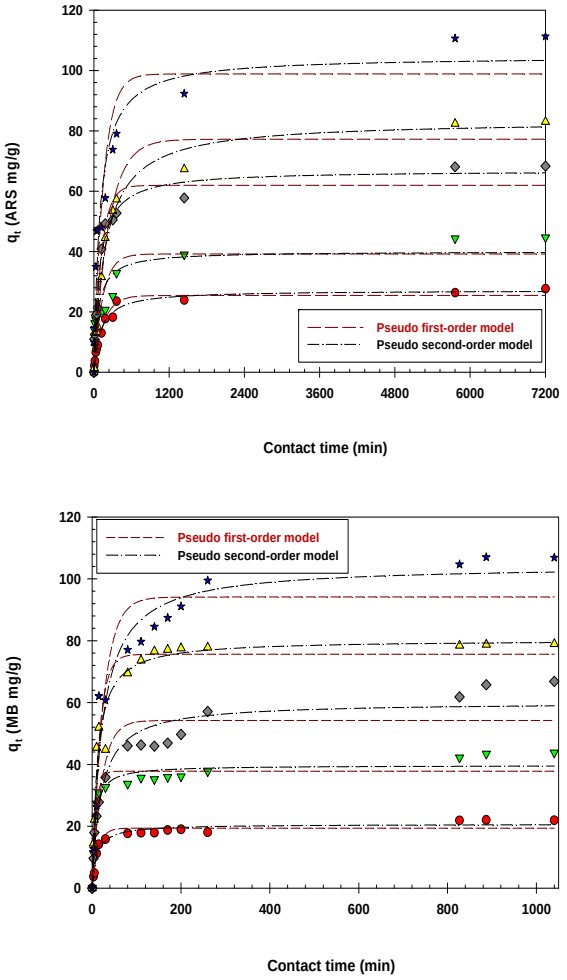

Figure 3: The fitting of pseudo first- and second-order models for ARS and MB removal onto OS.

From Table 3, the pseudo first- and pseudo second-order models fit the kinetic data with adequate accuracy. However, the experimental data demonstrated more agreement with the pseudo second-order model in terms of closer $q_{e,cal}$ values to $q_{e,exp}$ and higher correlation coefficients than the pseudo first-order model. This indicates that the chemical adsorption was the main control process for the olive stone (OS) material and the uptake capacity is proportional to the number of active sites [18]. The plots of q_t versus t and values of the constants of kinetic models obtained from the plots are given in Figure 3 and Table 3.

Table 3: Pseudo first-order and pseudo second-order model constants for ARS and MB adsorption onto olive stone.

	C_o		Pseudo first-order model			Pseudo second-order model		
		$q_{e,exp}$(mg/g)	$q_{e,cal}$ (mg/g)	k_1 (1/min)	R^2	$q_{e,cal}$ (mg/g)	k_2 (g/mg min)	R^2
ARS	**32 (mg/dm^3)**	27.64	25.43	0.004	0.968	27.16	3.0×10^4	0.983
	53 (mg/dm^3)	44.68	39.21	0.007	0.609	40.08	4.0×10^4	0.755
	87 (mg/dm^3)	68.32	61.95	0.008	0.947	66.91	2.0×10^4	0.971
	125 (mg/dm^3)	83.04	77.23	0.004	0.979	83.42	6.4×10^5	0.987
	190 (mg/dm^3)	111.32	98.89	0.006	0.877	104.7	9.9×10^5	0.947
MB	**29 (mg/dm^3)**	21.91	19.39	0.074	0.944	20.67	0.005	0.962
	60 (mg/dm^3)	43.77	37.80	0.118	0.929	39.68	0.001	0.952
	95 (mg/dm^3)	66.85	54.20	0.046	0.873	60.07	0.001	0.942
	137 (mg/dm^3)	78.96	75.60	0.064	0.941	80.26	0.001	0.967
	205 (mg/dm^3)	106.9	97.12	0.040	0.921	104.4	4.0×10^4	0.961

3.4. Biosorption Diffusion

The diffusion models were developed to study the diffusion of adsorbate inside the adsorbents. The first hypothesis used in these models is that the bulk liquid diffusion is not a limiting step which implies that stirring energy is sufficient. In this study the most common diffusion model in adsorption field was used: the intraparticle diffusion model. This model was employed in order to differentiate the different resistances toward diffusion of both MB and ARS adsorption onto olive stone. It links the pollutant adsorbed at a given time with the time t following the Equation **Error! Reference source not found.**:

$$q_t = k_{di} t^{0.5} \quad (5)$$

k_{di}, the intraparticle diffusion rate is constant and expressed in mg/g^1.h$^{0.5}$ where i represents the diffusion phase number. The plot of q_t versus t is linear when the intraparticle diffusion is the main resistance step in the experimental conditions. Generally the intraparticle diffusion rate is constant over a period of time at initial condition only. In fact several regions can usually be noticed in the diffusion of pollutants in porous materials [2]. The presence of different linear regions in the plot of q_t versus t is usually assumed to show the predominant of the resistance to diffusion of one process over another, i.e. pore diffusion, intraparticle diffusion, surface diffusion or the adsorption step itself. The tool developed by Malash and El-Khaiary was used to optimized the determination of the different intraparticle diffusion coefficient [19]. In Figure the diffusion of both MB and ARS at two different concentrations is presented. It can be seen that MB diffuses faster than ARS at both low and high concentration.

Table.

At low concentration the difference is more noticeable and MB is following a 3 steps diffusion process while ARS is following a 2 step diffusion process. The difference in diffusion steps can be related to the difference in the chemical charges of the 2 dyes. The higher charge density of MB compared to ARS enables a faster diffusion in OS.

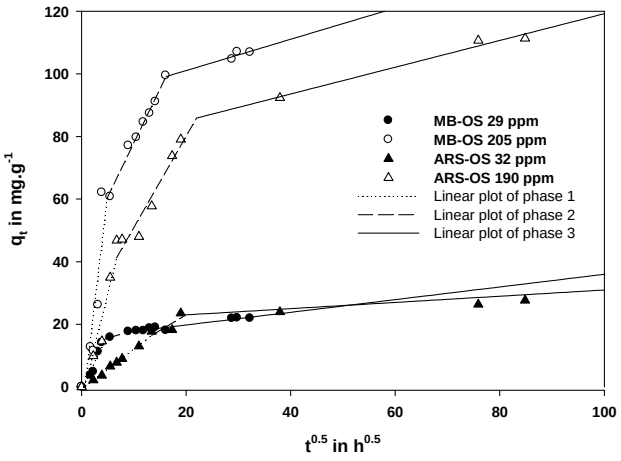

Figure 4: Intraparticle diffusion model applied to MB and ARS adsorption onto Olive Stone (OS).

In terms of diffusion parameters the difference between MB and ARS adsorption is clearly noticed for the first intraparticle diffusion step. The first step diffusion coefficients are more than double for MB adsorption than that for ARS adsorption,

Table 4: Intraparticle diffusion model parameters for the different diffusion phase

	Dye concentration	Intraparticle diffusion coefficients in mg/g.h$^{0.5}$					
Adsorbent	ppm	k_{d1}	r^2	k_{d2}	r^2	k_{d3}	r^2
MB-OS	29	3.74	0.92	0.51	0.95	0.20	0.88
MB-OS	205	14.06	0.75	3.45	0.99	0.50	0.47
ARS-OS	32	1.27	0.99	0.99	0.61	0.99	0.97
ARS-OS	190	6.71	0.93	2.92	0.94	0.43	0.98

4. REFERENCES

[1] Maria Visa, Cristina Bogatu, A. Duta, Simultaneous adsorption of dyes and heavy metals from multicomponent solutions using fly ash, Applied Surface Science, 256 (2010) 5486-5491.

[2] B. Noroozi, G.A. Sorial, Applicable models for multi-component adsorption of dyes: A review, Journal of Environmental Sciences, 25 (2013) 419-429.

[3] George Z. Kyzas, Nikolaos K. Lazaridis, M. Kostoglou, On the simultaneous adsorption of a reactive dye and hexavalent chromium from aqueous solutions onto grafted chitosan, Journal of Colloid and Interface Science, 407 (2013) 432-441.

[4] Y.S. Al-Degs, A.H. El-Sheikh, M.A. Al-Ghouti, B. Hemmateenejad, G.M. Walker, Solid-phase extraction and simultaneous determination of trace amounts of sulphonated and azo sulphonated dyes using microemulsion-modified-zeolite and multivariate calibration, Talanta, 75 (2008) 904-915.

[5] G. Blázquez, M. Calero, A. Ronda, G. Tenorio, M.A. Martín-Lara, Study of kinetics in the biosorption of lead onto native and chemically treated olive stone, Journal of Industrial and Engineering Chemistry, 20 (2014) 2754-2760.

[6] Silvina Pirillo, María Luján Ferreiraa, E.H. Ruedaa, The effect of pH in the adsorption of Alizarin and Eriochrome Blue Black R onto iron oxides, Journal of Hazardous Materials, 168 (2009) 168–178.

[7] L. Ai, Y. Zhou, J. Jiang, Removal of methylene blue from aqueous solution by montmorillonite/CoFe2O4 composite with magnetic separation performance, Desalination, 266 (2011) 72-77.

[8] A.B. Albadarin, J. Mo, Y. Glocheux, S. Allen, G. Walker, C. Mangwandi, Preliminary investigation of mixed adsorbents for the removal of copper and methylene blue from aqueous solutions, Chemical Engineering Journal, 255 (2014) 525-534.

[9] F. Banat, S. Al-Asheh, L. Al-Makhadmeh, Evaluation of the use of raw and activated date pits as potential adsorbents for dye containing waters, Process Biochemistry, 39 (2003) 193-202.

[10] M. Ghaedi, A. Hassanzadeh, S.N. Kokhdan, Multiwalled carbon nanotubes as adsorbents for the kinetic and equilibrium study of the removal of Alizarin red S and morin, Journal of Chemical and Engineering Data, 56 (2011) 2511-2520.

[11] A. Gürses, Ç. Doğar, M. Yalçın, M. Açıkyıldız, R. Bayrak, S. Karaca, The adsorption kinetics of the cationic dye, methylene blue, onto clay, Journal of Hazardous Materials, 131 (2006) 217-228.

[12] P. Janoš, H. Buchtová, M. Rýznarová, Sorption of dyes from aqueous solutions onto fly ash, Water Research, 37 (2003) 4938-4944.

[13] C. Namasivayam, S. Sumithra, Removal of direct red 12B and methylene blue from water by adsorption onto Fe (III)/Cr (III) hydroxide, an industrial solid waste, Journal of Environmental Management, 74 (2005) 207-215.

[14] C.D. Woolard, J. Strong, C.R. Erasmus, Evaluation of the use of modified coal ash as a potential sorbent for organic waste streams, Applied Geochemistry, 17 (2002) 1159-1164.

[15] Z. Wu, I.-S. Ahn, C.-H. Lee, J.-H. Kim, Y.G. Shul, K. Lee, Enhancing the organic dye adsorption on porous xerogels, Colloids and Surfaces A: Physicochemical and Engineering Aspects, 240 (2004) 157-164.

[16] Z. Wu, H. Joo, I.-S. Ahn, S. Haam, J.-H. Kim, K. Lee, Organic dye adsorption on mesoporous hybrid gels, Chemical Engineering Journal, 102 (2004) 277-282.

[17] J.-G. Yu, X.-H. Zhao, H. Yang, X.-H. Chen, Q. Yang, L.-Y. Yu, J.-H. Jiang, X.-Q. Chen, Aqueous adsorption and removal of organic contaminants by carbon nanotubes, Science of The Total Environment, 482–483 (2014) 241-251.

[18] Weifeng Liu, Jian Zhang, Cheng Cheng, Guipeng Tian, C. Zhang, Ultrasonic-assisted sodium hypochlorite oxidation of activated carbons for enhanced removal of Co(II) from aqueous solutions Original Research Article, Chemical Engineering Journal, 175 (2011) 24-32.

[19] G.F. Malash, M.I. El-Khaiary, Piecewise linear regression: A statistical method for the analysis of experimental adsorption data by the intraparticle-diffusion models, Chemical Engineering Journal, 163 (2010) 256-263.